Universal flow diagram for the magnetoconductance in disordered GaAs layers

S. S. Murzin,[1,2] M. Weiss,[1] A. G. M. Jansen,[1] and K. Eberl[3]
[1]*Grenoble High Magnetic Field Laboratory, Max-Planck-Institut für Festkörperforschung and Centre National de la Recherche Scientifique, Boîte Postale 166, F-38042 Grenoble Cedex 9, France*
[2]*Institute of Solid State Physics RAS, 142432 Chernogolovka, Moscow District, Russia*
[3]*Max-Planck-Institut für Festkörperforschung, Postfach 800 665 D-70569 Stuttgart, Germany*
(Received 18 September 2002; published 31 December 2002)

The temperature driven flow lines of the diagonal and Hall magnetoconductance data (G_{xx},G_{xy}) are studied in heavily Si-doped, disordered GaAs layers with different thicknesses. The flow lines are quantitatively well described by a recent universal scaling theory developed for the case of particle-vortex duality symmetry. The separatrix $G_{xy}=0.5$ (in units e^2/h) separates an insulating state from a quantum Hall-effect (QHE) state. The merging into the insulator or the QHE state at low temperatures happens along a semicircle separatrix $G_{xx}^2+(G_{xy}-1/2)^2=1/4$, which is divided by an unstable fixed point at $(G_{xx},G_{xy})=(1/2,1/2)$.

DOI: 10.1103/PhysRevB.66.233314 PACS number(s): 73.50.Jt, 73.61.Ey, 73.43.−f

In spite of considerable efforts in theoretical and experimental research on the quantum hall effect (QHE) for many years, the complete description of its phase diagram and evolution for decreasing temperature is still unsatisfactory at the moment. About 20 years ago, a flow diagram[1] for the coupled evolution of the diagonal (G_{xx}) and Hall (G_{xy}) conductivities was sketched for increasing sample size L (or, equivalently, increasing phase breaking length L_ϕ for finite decreasing temperatures) on the basis of a two-parameter scaling approach to the QHE.[2] With increasing system size $(L\to\infty)$, the points $[G_{xx}(L),G_{xy}(L)]$ flow on lines merging into the QHE plateau states characterized by the fixed points $(0,i)$, where i is an integer with G_{xx} and G_{xy} in units e^2/h. In addition, there are unstable fixed points in between these plateaus at $(G_{xx}^c,G_{xy}^c=i+1/2)$, where the flow lines terminate, meaning that points with $G_{xy}=i+1/2$ maintain their Hall conductance for all L. More recently, quantitative estimates for the flow diagram have been given for the case of noninteracting electrons: for different random potentials at high magnetic field in the lowest Landau level numerical calculations give $G_{xx}^c\approx 1/2$ (Ref. 3) and for a smooth disorder potential at sufficiently low temperatures, the (G_{xx},G_{xy}) data have been derived to flow on a separatrix in the form of a semicircle,[4]

$$G_{xx}^2+[G_{xy}-(i+1/2)]^2=1/4, \tag{1}$$

with $G_{xx}^c=1/2$ and $G_{xy}^c=i+1/2$.

Although, QHE experiments reveal certain aspects of the two-parameter scaling behavior, the picture is not yet fully confirmed. Magnetotransport studies of the flow diagram[5] clearly demonstrate the quantization of G_{xy} but do not show essential features of the two-parameter scaling picture like the symmetry with respect to the vertical lines $G_{xy}=i$ and $i+1/2$ or the correct values of $G_{xx}^c=1/2$ and $G_{xy}^c=i+1/2$. Moreover, in a series of papers,[6] the observation of a transition from the insulating state $(i=0)$ directly into high-integer QHE states with $i\geqslant 2$ has been reported. This is inconsistent with the proposed phase diagram of the QHE which is derived on the basis of the two-parameter-scaling picture.[7]

The similarity of many features of the fractional and integer QHE stimulated the creation of a unified theory involving the composite fermion picture.[7,8] This development, making use of particle-vortex duality and particle-hole symmetries,[9] very recently resulted in the derivation of exact expressions for the flow lines of the integer and fractional QHE.[10] Their shape is universal, i.e., it does not depend on any parameters of the 2D system. The separatrix are the above given semicircles and the vertical lines $G_{xy}=i+1/2$. The flow diagram of the integer QHE can be mapped into the diagram of the fractional QHE using a simple algebraic transformation.[9,10]

In the present work, we explore the temperature driven flow diagram of $G_{xx}(T)$ versus $G_{xy}(T)$ for disordered, heavily Si-doped GaAs layers with different thicknesses from 40 to 27 nm in a large-temperature range from 4.2 K down to 40 mK. At low temperatures, these samples are situated in the transition region between a QHE state and an insulating state. The temperature evolution of the (G_{xx},G_{xy}) data points of these disordered samples shows a complete quantitative agreement with the universal theory[10] for the flow diagram.

The theory introduced in Ref. 10 has been developed for spinless (or totally spin polarized) electrons. Therefore, the most favorable candidate for an experimental study of the flow diagram under integer QHE conditions is a disordered system with a small g factor such that the spin splitting $\mu_B gB$ (μ_B is the Bohr magneton) is small with respect to the disorder broadening and will only show up in the flow diagram at rather low temperatures.[11] As we have shown in previous investigations on similar samples, electron-electron interaction cannot be neglected in the systems that are subject of the present work.[12] For $G_{xx}>1$, interaction mainly leads to temperature-dependent flow of the $[G_{xx}(T),G_{xy}(T)]$ data[13] and a dependence of the localization length on interaction.[12] For $k_BT\ll\mu_B gB$ (k_B is the Boltzmann constant), only interaction of electrons with the same spin leads to a renormalization of the conductance.[14] Therefore, under these conditions and in the absence of spin-flip scattering, electrons with different spin can be considered as two independent, totally spin-polarized electron systems. For such a

situation, one should compare the theory with the measured conductivity per spin $G_{ij}^{\uparrow}=G_{ij}/2$.

The disordered GaAs samples were prepared by molecular-beam epitaxy. On a GaAs (100) substrate were successively grown an undoped GaAs layer (0.1 μm), a periodic structure of 30 $\times$GaAs/AlGaAs (10/10 nm), an undoped GaAs layer (0.5 μm), the heavily Si-doped GaAs layer of a nominal thickness of $d=27$, 30, 34, and 40 nm, and with a Si-donor concentration of 1.5×10^{17} cm^{-3}, followed by a cap layer of 0.5 μm undoped GaAs. The number given for a sample corresponds to the thickness of its doped layer. Hall bar geometries of width 0.2 mm and length 2.8 mm were etched out of the wafers. A phase-sensitive ac technique was used for the magnetotransport measurements down to 40 mK with the applied magnetic field up to 12 T perpendicular to the layers. For samples 27 and 30, the absolute values of the Hall resistance R_{xy} were about 10% different for two opposite directions of the magnetic field. The average has been taken as R_{xy}. The electron densities per square as derived from the slope of the Hall resistance R_{xy} in weak magnetic fields (0.5–3 T) at T=4.2 K are $N_s=3.7$, 4, 5.5, and 6.2×10^{11} cm^{-2} for samples 27, 30, 34, and 40, respectively. The ''bare'' high-temperature mobilities μ_0 are about 1300,1400,1900, and 2300 cm^2/Vs. Because of the rather large quantum corrections to the conductivity, even in zero magnetic field at 4.2 K, we used the approximate relation $\mu_0=R_{xy}/BR_{xx}$ in the intersection point of the $R_{xx}(B)$ curves for different temperatures. Previous experimental studies of the flow diagram have been performed on much purer samples with mobilities at least an order of magnitude higher.

Samples 34 and 40 reveal a wide QHE plateau from ≈6 up to ≈11 T with the value $R_{xy}=1/2$ (i.e., $i=2$ for a spin degenerate lowest Landau-level occupation) accompanied by an exponentially small value of R_{xx} at low temperatures $T\lesssim0.3$ K. The magnetoresistance data of sample 40 are presented in Ref. 12.

In Fig. 1, the magnetotransport data of the diagonal (R_{xx}, per square) and Hall (R_{xy}) resistance (both given in units of h/e^2), and of the diagonal (G_{xx}) and Hall (G_{xy}) conductance have been plotted for sample 30. At $T=4.2$ K, R_{xx} depends on magnetic field rather weakly and has only a weak minimum at $B=6$ T, and R_{xy} increases linearly up to 5 T with a slightly smaller slope at higher fields. Such a behavior is typical for bulk samples in the extreme quantum limit. At the lowest temperatures, the layer is insulating ($R\geqslant100$) in zero magnetic field. At low magnetic fields up to 0.5 T, the diagonal resistance R_{xx} drops abruptly and continues to decrease more slowly between 0.5 and 4 T. For fields between 5 and 7 T, a minimum is observed with a QHE plateau in the Hall resistance with $R_{xy}=1/2$. The same QHE structure around 6 T can be observed in the plotted conductance data. In the minimum of G_{xx} near $B=6$ T, the Hall conductance G_{xy} increases from a value higher than 1 (at 4.2 K) towards 2 at the lowest temperatures. The curves $G_{xy}(B)$ for different temperatures cross at one point with $G_{xy}=1$ at $B_c=4.9$ T. The diagonal conductivity tends towards 1 for decreasing temperature at this critical field. For curves at $T>0.2$ K,

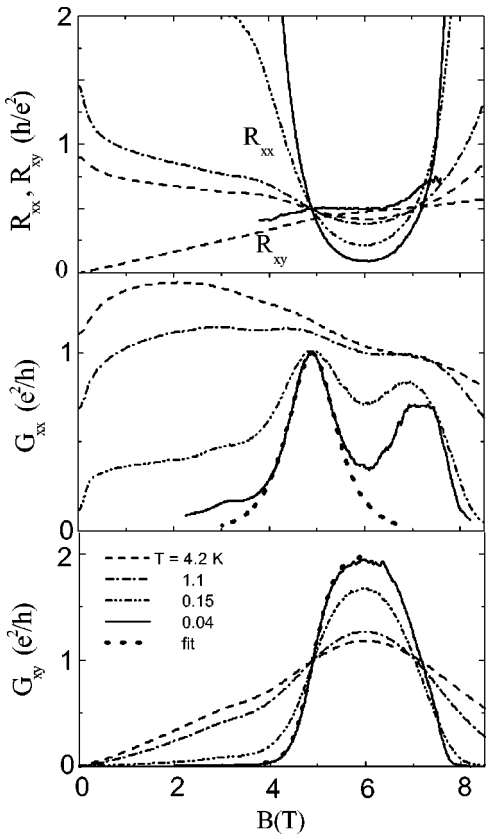

FIG. 1. Magnetic-field dependence of the diagonal (R_{xx}, per square) and Hall (R_{xy}) resistance and the diagonal (G_{xx}) and Hall (G_{xy}) conductance for sample 30 in a magnetic field perpendicular to the heavily doped GaAs layer at different temperatures. Dotted lines for G_{xx} and G_{xy} show the result of a theoretical fit by Eq. (4) around $B_c=4.9$ T.

there is a second crossing point at $B=7$ T with $G_{xy}\approx1$. The second peak in $G_{xx}(B)$ has an amplitude smaller than 1 and is broader than the first one. We believe that this peculiar structure of the second peak is a manifestation of spin splitting.

In Fig. 2, the magnetotransport data have been plotted for sample 27. At $T=4.2$ K, these data are similar to the data for sample 30. However, sample 27 shows insulating behavior (R_{xx} increases with decreasing temperature) at all magnetic fields with a rather deep and narrow minimum in the field dependence $R_{xx}(B)$ at low temperatures. Note that at the lowest temperature, we can measure R_{xy} only near the minimum of R_{xx} since outside this region, $R_{xy}\ll R_{xx}$. Within our accuracy, the sample reveals a Hall-insulator state ($R_{xy}=0.5$, Ref. 7) in this region. G_{xx} and G_{xy} have peaks at $B\approx6$ T.

The QHE in sample 30 is much less pronounced than in samples 34 and 40 due to the fact that the maximum of the high-temperature Hall conductance $G_{xy}^0(B)$ has a value of ≈1.2 close to 1 (see Fig. 1). For $G_{xy}^0\rightarrow1$, the localization length diverges, and the system is in the dissipative, nonquantized state. For samples 34 and 40 with a maximum of $G_{xy}^0(B)$ close to 2, quantization at $G_{xy}=2$ develops already at higher temperatures. Although insulating for all fields,

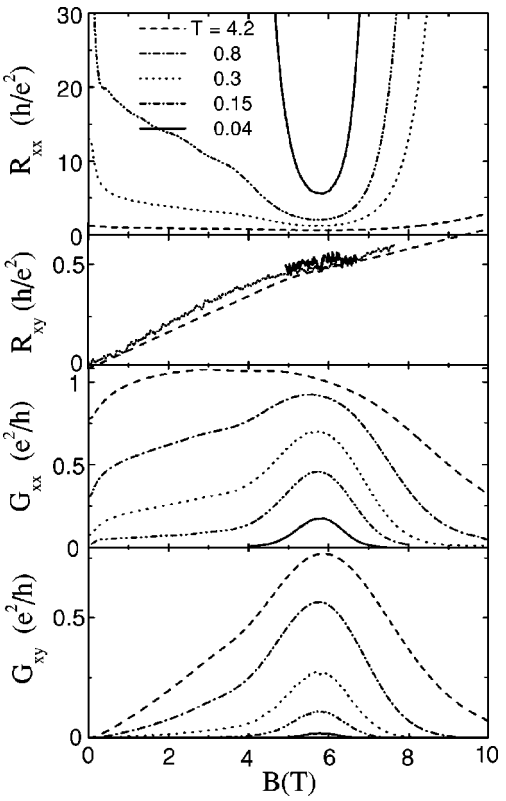

FIG. 2. Magnetic-field dependence of the diagonal (R_{xx}, per square) and Hall (R_{xy}) resistance, and diagonal (G_{xx}) and Hall (G_{xy}) conductance for sample 27 in a magnetic field perpendicular to the heavily doped GaAs layer at different temperatures.

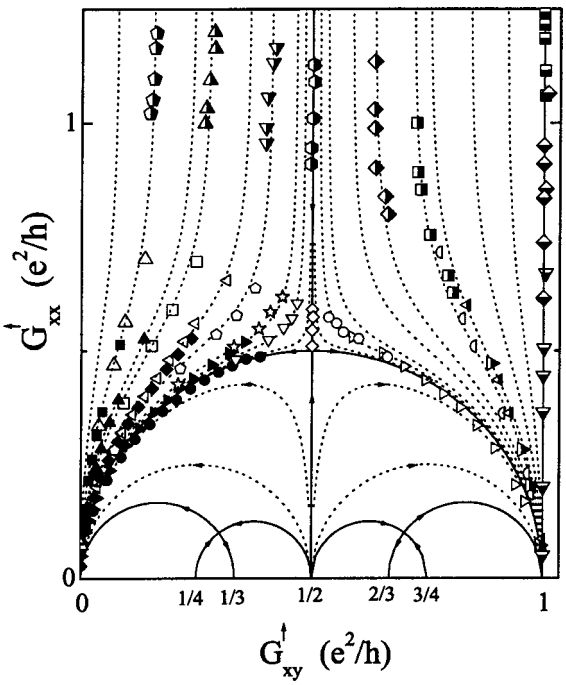

FIG. 3. Flow diagram of the $[G_{xx}^{\uparrow}(T), G_{xy}^{\uparrow}(T)]$ data points for the investigated heavily doped GaAs layers with different thickness. Filled symbols, sample 27 ($B=1.7$–6.1 T); open, sample 30 ($B=1.62$–5.8 T); half right filled, sample 34 ($B=0.9$–5.8 T); and half bottom filled, sample 40 ($B=3.3$–6 T). Different magnetic-field values are indicated by different types of symbols. Dotted lines show the theoretical flow lines. Solid lines display the separatrix for the integer and partially for the fractional QHE.

sample 27 shows a minimum in R_{xx} and a maximum in G_{xx} due to the proximity of $G_{xy}^{0}(B)$ to 1 on the insulator side, giving a large localization length at its maximum.

In Fig. 3, the temperature evolution of the points $[G_{xx}^{\uparrow}(T), G_{xy}^{\uparrow}(T)]$ of the conductance per spin $G_{ij}^{\uparrow}=G_{ij}/2$ has been plotted for the different samples at different magnetic fields with temperature ranging from 4.2 down to 0.04 and 0.1 K except for the flow lines of sample 34 in weak magnetic fields (1.4–2.4 T) which start only at 1.1 K. Only data below $B=6.2$ T have been plotted because in higher magnetic fields, spin splitting starts to affect the magnetotransport properties. A distinct signature of spin splitting has been observed in samples 40 and 34, and will be subject of a separate publication. The data points at the lowest temperatures approach and, subsequently, follow the semicircle dependence given in Eq. (1). Their final low-temperature limiting value depends on the initial high-temperature Hall conductance $G_{xy}^{\uparrow 0}$ with respect to $G_{xy}^{\uparrow}=1/2$. Data points starting on the semicircle follow this semicircle. The points starting for high temperatures at $G_{xy}^{\uparrow}=1/2$ terminate at the lowest temperatures very close to $(G_{xx}^{c}, G_{xy}^{c})=(1/2,1/2)$. The presented data on disordered GaAs layers follow the trends expected from universal scaling arguments.

In the following, we will give a quantitative estimate for the temperature-dependent evolution of the flow lines at constant magnetic field. The dotted flow lines in Fig. 3 are plotted as a result of a numerical solution of the equation $\arg(f)=\alpha$ for various α, where

$$f=-\vartheta_3^4\vartheta_4^4/\vartheta_2^8, \tag{2}$$

with the Jacobi ϑ functions

$$\vartheta_2(q)=2\sum_{n=0}^{\infty} q^{(n+1/2)^2}, \quad \vartheta_3(q)=\sum_{n=-\infty}^{\infty} q^{n^2},$$

$$\vartheta_4(q)=\sum_{n=-\infty}^{\infty} (-1)^n q^{n^2}, \tag{3}$$

for $q=\exp[i\pi(G_{xy}+iG_{xx})/2]$.[10] The value α corresponds to the Hall conductance G_{xy}^{∞} for large G_{xx}, where the flow lines are vertical, with $\alpha=\pi(1-G_{xy}^{\infty})$ [for the flow lines above the semicircle Eq. (1)]. The theoretical flow lines are in a very good agreement with the experimental data and are universally determined by the limiting G_{xy}^{∞} values. Note that solutions of the above equations contain the flow lines for the fractional QHE as well.

The rate of flow with decreasing temperature is determined by the parameter $s-s_0=\ln(f/f_0)$, where $f_0=f(s_0)$.

For flow along the semicircle from the critical point, where $f_0=1/4$, we have $s=\ln(4f)$. In this case,[10] for total conductivity

$$G_{xx}=2\frac{K'(w)K(w)}{K(w)^2+K'(w)^2},\quad G_{xy}=2\frac{K'(w)^2}{K(w)^2+K'(w)^2},$$

$$w=\sqrt{\frac{1\pm[1-\exp(-s)]^{1/2}}{2}}, \tag{4}$$

where $K(w)$ is the complete elliptic function of the second kind, with $K'(w)\equiv K(\sqrt{1-w^2})$. The temperature dependence of G_{xx} and G_{xy} along the semicircle for samples 27, 30, and 40 can be fitted by Eq. (4) and $s=c/T^p$ (with T in kelvin) with $p=1.16$, 0.94, 1.1 ± 0.1 and $c=0.83,0.58,3.5$, correspondingly. As shown in Fig. 1 the data for $G_{xx}(B)$ and $G_{xy}(B)$ of sample 30 at the lowest temperature are well described by Eq. (4) and $s=22(\Delta B)^2$ (with ΔB in tesla) around the critical point $B_c=4.9$ T.

As is mentioned above, for $k_BT\ll\mu_BgB$, only interaction of electrons with the same spin leads to a renormalization of the conductance. In our experiments, $\mu_BgB/k_BT=0.01$–3. It seems that even for $k_BT\gtrsim\mu_BgB$, the flow lines remain unchanged while the interaction of electrons with different spin effects can be important for the flow rate.

For large values of G_{xx}, its temperature dependence is mostly due to electron-electron interaction and the parameter s can be written as $s=(\lambda/\pi)\ln L_T$, where L_T is the coherence length for interaction and the constant of interaction λ is a material parameter that depends on magnetic field ($\lambda<1$). Note that compared to the two-parameter scaling theory, L_ϕ is replaced by L_T. The interaction effects accelerate the motion along the lines.

In summary, the flow diagram of $[G_{xx}(T),G_{xy}(T)]$ data for strongly disordered GaAs layers is well described by the universal expressions following from duality and particle-hole symmetries. Electron-electron interaction leads to an accelerated flow rate but does not change the shape of the flow lines.

This work was supported by RFBR and INTAS. We would like to thank B. Lemke for her help in the preparation of the samples.

[1] D.E. Khmel'nitskiĭ, Pis'ma Zh. Éksp. Teor. Fiz. **38**, 454 (1983) [JETP Lett. **38**, 552 (1983)]; Phys. Lett. A **106**, 182 (1984).
[2] H. Levine, S.B. Libby, and A.M.M. Pruisken, Phys. Rev. Lett. **51**, 1915 (1983); A.M.M. Pruisken, Nucl. Phys. B: Field Theory Stat. Syst. **235[FS11]**, 277 (1984); Phys. Rev. B **32**, 2636 (1985).
[3] Y. Huo, R.E. Hetzel, and R.N. Bhatt, Phys. Rev. Lett. **70**, 481 (1993).
[4] Igor Ruzin and Shechao Feng, Phys. Rev. Lett. **74**, 154 (1995).
[5] H.P. Wei *et al.*, Phys. Rev. B **33**, 1488 (1988); Surf. Sci. **229**, 34 (1990); Phys. Rev. B **45**, 3926 (1992); M. Yamane *et al.*, J. Phys. Soc. Jpn. **58**, 1899 (1989); S.V. Kravchenko *et al.*, Pis'ma Zh. Eksp. Teor. Fiz. **50**, 65 (1989) [JETP Lett. **50**, 73 (1989)] ; S. Koch *et al.*, Phys. Rev. B **43**, 6828 (1991); V.T. Dolgopolov *et al.*, Zh. Eksp. Teor. Fiz. **99**, 201 (1991) [Sov. Phys. JETP **72**, 113 (1991)].
[6] V.M. Pudalov *et al.*, Pis'ma Zh. Éksp. Teor. Fiz. **57**, 592 (1993) [JETP Lett. **57**, 608 (1993)]; S. Kravchenko *et al.*, Phys. Rev. Lett. **75**, 910 (1995); S.-H. Song *et al.*, *ibid.* **78**, 2200 (1997); S.C. Dultz *et al.*, Phys. Rev. B **58**, 7532 (1998); C. Lee *et al.*, *ibid.* **58**, 10 629 (1998); M. Hilke *et al.*, *ibid.* **62**, 6940 (2000); C.F. Huang *et al.*, *ibid.* **65**, 045303 (2002).
[7] S. Kivelson, D. Lee, and S. Zang, Phys. Rev. B **46**, 2223 (1992).
[8] J.K. Jain, Phys. Rev. Lett. **63**, 199 (1989).
[9] C.P. Burgess and B.P. Dolan, Phys. Rev. B **63**, 155309 (2001).
[10] B.P. Dolan, Nucl. Phys. B: Field Theory Stat. Syst. **460**[FS], 297 (1999); cond-mat/9809294.
[11] D.E. Khmel'nitskiĭ, Helv. Phys. Acta **65**, 164 (1992).
[12] S.S. Murzin, M. Weiss, A.G.M. Jansen, and K. Eberl, Phys. Rev. B **64**, 233309 (2001).
[13] S.S. Murzin, Pis'ma Zh. Éksp. Teor. Fiz. **67**, 201 (1998) [JETP Lett. **67**, 216 (1998)].
[14] A.M. Finkelstein, Zh. Éksp. Teor. Fiz. **86**, 367 (1984) [Sov. Phys. JETP **59**, 212 (1984)].